

Title

Subtitle

by

Mikkel Metzsch Jensen

THESIS

for the degree of

MASTER OF SCIENCE



Faculty of Mathematics and Natural Sciences
University of Oslo

Spring 2023

Title

Subtitle

Mikkel Metzsch Jensen

© 2023 Mikkel Metzsch Jensen

Title

<http://www.duo.uio.no/>

Printed: Reprosentralen, University of Oslo

Abstract

Abstract.

Acknowledgments

Acknowledgments.

Contents

List of symbols?	vii
Introduction	1
0.1 Motivation	1
0.1.1 Friction	1
0.1.2 Thesis	1
0.2 Approach	1
0.3 Objective of the study	2
0.4 Contributions	2
0.5 Thesis structure	2
Simulations	3
0.5.1 Baseline	5
0.5.1.1 Single measurement	5
0.5.1.2 Defining metrics for dynamic and static friction	8
0.5.1.3 Varying temperature, drag speed, spring constant and dt	11
0.5.1.4 Varying normal force and stretch	13
0.5.1.5 Contact area	15

List of symbols?

Maybe add list of symbols and where they are used like Trømborg.

Introduction

0.1 Motivation

0.1.1 Friction

Friction is a fundamental force that takes part in almost all interactions with physical matter. Even though the everyday person might not be familiar with the term “friction” we would undoubtedly notice its disappearing. Without friction, it would not be possible to walk across a flat surface, lean against the wall or secure an object by the use of nails or screws (Static friction allows us to join objects together using screws [1][p. 5]). Similarly, we expect a moving object to eventually come to a stop if not supplied with new energy, and we know intuitively that sliding down a snow covered hill is much more exciting than its grassy counterpart. It is probably safe to say that the concept of friction is well integrated in our everyday life to such an extent that most people take it for granted. However, the efforts to control friction dates back to the early civilization (3500 B.C.) with the use of the wheel and lubricants to reduce friction in translational motion [2]. Friction is a part of the wider field tribology derived from the Greek word *Tribos* meaning rubbing and includes the science of friction, wear and lubrication [2].

The most important motivation to study tribology is ultimately to gain full control of frictional and wear for various technical applications. Especially, reducing friction is of great interest as this has tremendous advantages regarding energy efficiency. It has been reported that that monetary value of tribological problems has significant potential for economic and environmental improvements [3]:

“On global scale, these savings would amount to 1.4% of the GDP annually and 8.7% of the total energy consumption in the long term.” [4].

The reduction of friction is not the only sensible application as a controlled increase in friction might be of interest in the development of grasping robots or perhaps braking system (get some sourced examples maybe...).

0.1.2 Thesis

In this thesis we investigate the possibility to control the frictional properties of a graphene sheet by applying strategically positioned cuts to the sheet inspired by kirigami. Kirigami is a variation of origami where the paper is cut additionally to being folded. Hanakata et al. [5] has shown that kirigami inspired cuts on a graphene sheet can be used to alter the yield strain and yield stress of the sheet. They observed that the stretching of the cutted sheet induced a out-of-plane buckling which serves as a key observation for the motivation of this thesis. It is currently well established/believed that the friction between two surfaces is proportional to the real microscopic contact area (source here?). Hence, one can hypothesize that the buckling of the sheet will affect the contact area and consequently the frictional properties.

0.2 Approach

In the study by Hanakata et al. [5] they used a machine learning (ML) approach to overcome the complexity of the nonlinear effects arising from the out-of-plane buckling which made them successfully map the cutting patterns to the mechanical properties of yield and stress. The dataset used for the ML training was generated by molecular dynamics (MD) simulations for a limited set of cut configuration. By training the network the MD simulations could effectively be skipped all together making for an accelerated search through new cut configurations for certain mechanical properties. By setting up a MD simulation that quantifies the frictional

properties of the graphene sheet we aim to make an analog study regarding the search for certain frictional properties.

We will take this on step further by creating a GAN network that utilises the latter network for creating an inverse design framework. That is, a network that takes frictional properties as input and return the corresponding cut configuration. By having such a tool we can execute a targeted search for exotic frictional properties. Particularly, we are interested in nonlinear and possibly even negative friction coefficients. Friction is essentially observed to increase with increasing load on the frictional surface, and we often describe this as having a positive friction coefficient. However, if we are able to couple the stretching of the sheet with friction we might be able to break this barrier for the coefficient. By imagining some nanomachine which translates downward pressure into either compression or expansion of the altered graphene, we could have a coupling between downward pressure and stretch of the sheet. In that case, a friction force depending on stretch could effectively be made to decrease with increasing load which would correspond to a negative friction coefficient following this definition (formulate such that we do not imply free acceleration from nothing).

One of the features from inverse design, separating it from the general class of ML approaches, is that we do not depend on trusting the ML predictions. While a standard neural network might be extremely efficient on a certain prediction task we have usually no information on how these predictions are based. We say that the internal workings of the network is a black box beyond our capacity of interpretation. However, for the inverse design problem we are prompted with a few promising design proposals which can immediately be tested in the MD simulations which we will regard as the most reliable predictor in this setting. Hence, if arriving at a successful design in alignment our search prompt, we can disregard any uncertainty in the network. In that case the remaining gap to bridge is that of the MD simulation and real life implementations.

0.3 Objective of the study

1. Design a MD simulation to evaluate the frictional properties of the graphene sheet under different variations of cut patterns, stretching and loading, among other physical variables.
2. Train a network to replace the MD simulation completely.
3. (Variation 1) Do an accelerated search using the ML network for exotic frictional properties such as low and friction coefficients and a strong coupling between stretch and friction.
4. (Variation 2) Make a GAN network using the first network and predict cut configurations for some of the above mentioned frictional properties.
5. (If I have time) Make a nanomachine that couples load and stretch (perhaps just artificially without any molecular mechanism) to test the hypothesis of a negative friction coefficient.

0.4 Contributions

What did I actually achieve

0.5 Thesis structure

How is the thesis structured.

Simulations

Frictional properties of the intact graphene sheet

The friction measurement simulation is governed by the following parameters, which is divided into three sub categories for the purpose of this thesis as shown in table [1](#).

Table 1: Parameters of the numerical procedure for measuring friction.

Category	Parameter name: description	Category purpose
Physical	<ul style="list-style-type: none"> - T: Temperature for the Langevin thermostat. - v_{drag}: Drag speed for the sheet translation. 	Parameters that we expect to have an inevitably effect on the system friction properties, for which the choice will be a baseline for our studies.
Measurement	<ul style="list-style-type: none"> - dt: Integration timestep. - t_R: Relaxtion time before strething. - Pauses between stretch and adding normal force and between dragging the sheet. - Stretch Speed: How fast to stretch the sheet. - K: Spring constant for the spring responsible of translating the sheet. An infinte spring constant is achieved by moving the end blocks as a rigid body (Lammps: fix move). - Drag Length: How far to translate the sheet. - Sheet size: Spatial size of the 2D sheet. 	Paramters that effects the simulation dynamics and the 'experimental procedure' that we a mimicking. We aim to choose to these paramters such that the friction properties is stable for small perturbations.
ML input	<ul style="list-style-type: none"> - Sheet configuration: A binary matrix containing information of which atoms is removed (0) and which is still present (1) in the graphene structure. - Scan angle: The direction for which we translate the sheet. - Stretch amount: The relative sheet stretch in percentage. - F_N: Applied normal force to the end blocks. 	The remaining paramters that serve as the governing variables in the optimization process for certain friction properties and is thus the input variables for the ML part.

We should try to set the phycsis and measurement parameters in such a way that we reduce computation speed where it is doesn't infer with the frictional properties study.

We need to define some ranges for the ML input paramters. F_N , stretch ranges where it is not prone to ruptures. The configuration it self does not have clear rules but is also being regulated by the no rupture requirement.

0.5.1 Baseline

0.5.1.1 Single measurement

Force oscillations We first assess the raw data for the friction force F_{\parallel} parallel to the drag direction as seen in figure 1. The sample rate is 10 ps^{-1} for which we sample the the mean of all previous timesteps. We observe that the data carries oscillations on different time scales. By applying a savgol filter to data with a polyorder of 5 and window length corresponding to a drag length of 3.0 \AA (or time interval 15.0 ps) we can qualitatively point out at least two different frequencies of oscillation. On figure 1a we see roughly three waves on the savgol filter corresponding to one frequency, while on 1b the same savgol filter reveals an even slower frequency on top of the first creating a visual patterns of a wavepacket.

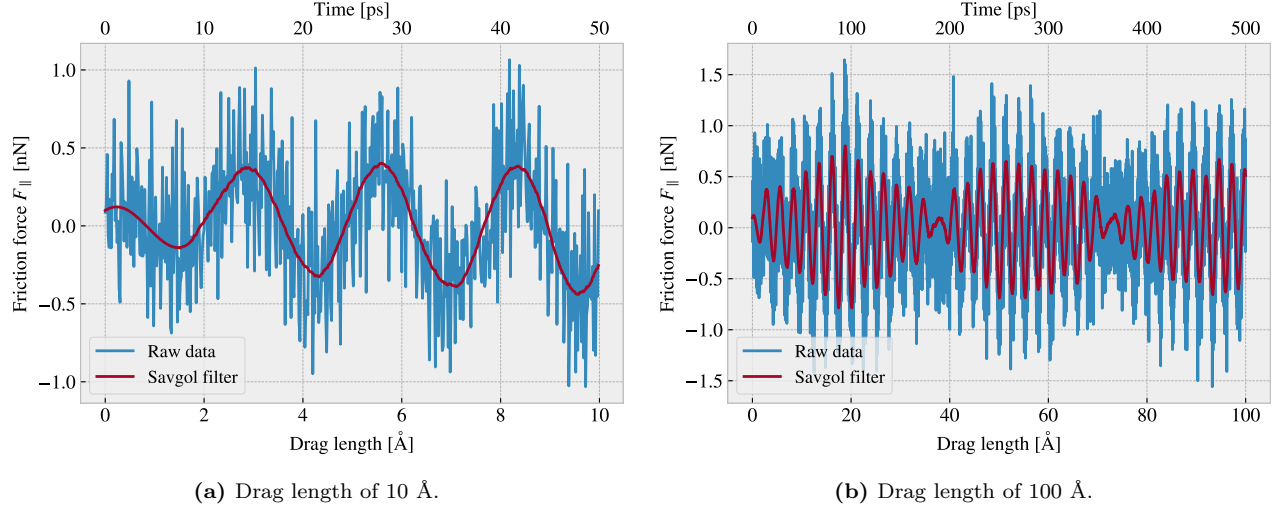


Figure 1: Friction force F_{\parallel} between (full) sheet and substrate with respect to the drag direction vs. drag length. The drag length is measured by the constant movement of the virtual atom and not the COM of the sheet. The red line represents a savgol filter with window polyorder 5 and window length 150 (corresponding to a drag length of 3 \AA or a time window of 15 ps)

By performing a Forward Fourier Transform of the data (using FFT) we can quantitatively identify some of the leading frequencies as seen in figure 2a. By plotting the two most dominant frequencies $f_1 = 0.0074 \text{ ps}^{-1}$ and $f_2 = 0.0079 \text{ ps}^{-1}$ as $\sin(2\pi f_1) + \sin(2\pi f_2)$ we find a convincing fit to the observed wavepacket shape as seen in figure 2b. By using the trigonometric identity

$$\begin{aligned}\sin(\alpha + \beta) &= \sin(\alpha) \cos(\beta) + \cos(\alpha) \sin(\beta), \\ \sin(\alpha - \beta) &= \sin(\alpha) \cos(\beta) - \cos(\alpha) \sin(\beta),\end{aligned}$$

and decomposing $f_1 = a - b$, $f_2 = a + b$ we can rewrite the sine sum as the sinusoidal product

$$\begin{aligned}\sin(2\pi f_1) \sin(2\pi f_2) &= \sin(2\pi(a - b)) \sin(2\pi(a + b)) \\ &= \sin(a) \cos(b) + \cancel{\cos(2\pi a) \sin(2\pi b)} + \sin(2\pi a) \cos(2\pi b) - \cancel{\cos(2\pi a) \sin(2\pi b)} \\ &= 2 \sin(2\pi a) \cos(2\pi b),\end{aligned}$$

with

$$\begin{aligned}a = \frac{f_1 + f_2}{2} &= 0.0763 \pm 0.0005 \text{ ps}^{-1}, & b = \frac{f_2 - f_1}{2} &= 0.0028 \pm 0.0005 \text{ ps}^{-1}, \\ &= 0.381 \pm 0.003 \text{ \AA}^{-1}, & &= 0.014 \pm 0.003 \text{ \AA}^{-1},\end{aligned}$$

where the latter frequency is denoted with respect to drag length. This makes us recognize the fast oscillation frequency as a and the slower frequency as b . We also take note of the longest period in the data $T_b = 1/b \sim 357 \text{ ps} \sim 71 \text{ \AA}^{-1}$ which will be relevant for the evaluation of measurement uncertainty.

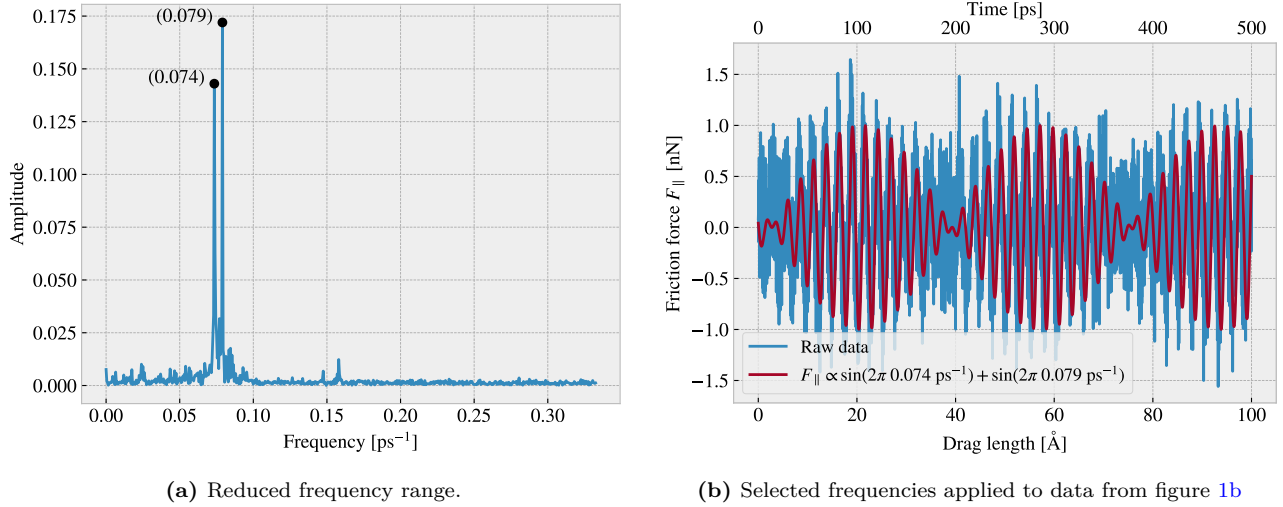


Figure 2: Fourier transform on data shown in figure 1.

Decompositions In the previous analysis we have looked only as the friction force for the full sheet, including the pullblocks which is locked off during the drag, and with respect to the drag direction.

Since we are only applying cuts to the inner sheet (excluding the pull blocks), it might seem more natural to only consider the friction on that part. If the desired frictional properties can be observed from the inner sheet we can always scale the relative size between inner sheet and pull block. However, when looking at the time series of friction force decomposed onto inner sheet and pull block (figure 3a) we observe the friction force arising from those parts is seemingly antisymmetric. That is, the frictional pull on the substrate is oscillating between the inner sheet and the pullblock. Remembering that the normal force is only applied to the pull block we might take this as an integrated feature of the system. An interesting nonlinear friction coefficient might depend on this internal distribution of forces. Hence, we hedge our bets and use the full sheet friction force as a holistic approach to the measurement problem.

Similar we might question the decision of only considering the frictional force projected on the direction of the drag as we are neglecting the “side shift” induced during the drag phase. In figure 3b we see the decomposition into force components parallel F_{\parallel} and perpendicular F_{\perp} to the drag direction respectively. We see that the most dominant trends is projected into the parallel component. If we want to include the perpendicular component as well we would have to evaluate the friction as the length of the vector for which we lose the sign of direction. Hence we would only get positive contributions, meaning a resisting force, which is not faithfully capturing the sheet oscillations that make the friction forces act both against and with the direction of drag. By this argument we decide to use only the parallel component going forward.

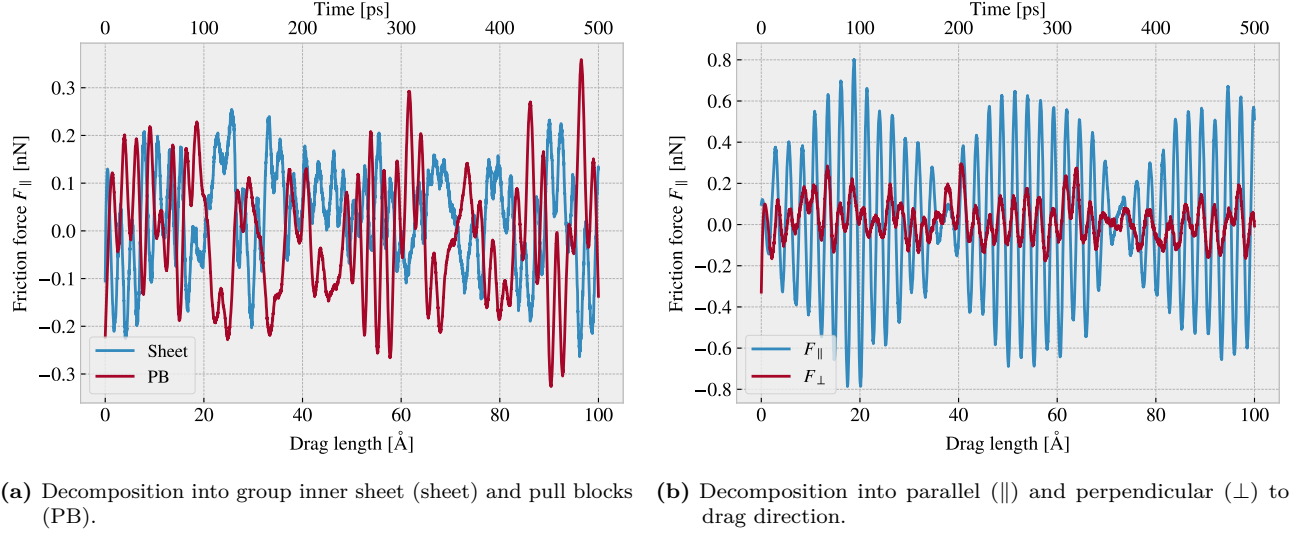


Figure 3: Decomposition into parallel (\parallel) and perpendicular (\perp) to drag direction showing the savgol filter applied

Center of mass path From the previous observations we already have evidence of a stick slip behaviour, judging from the friction oscillations in figure 1, and motion partial motion perpendicular to the drag direction, judging from the perpendicular force component in figure 3b. By looking at the x, y -position for the center of mass (COM) we can see the stick slip motion manifested as a variation in COM speed combined with a side to side motion as shown in figure 4a. To increase this effect we also show the same plot with a spring ... move with spring constant 30 N/m in figure 4b. While the max speed is on the same scale the side to side motion is increased (notice that the axis scale is different between figure 4a and 4a).

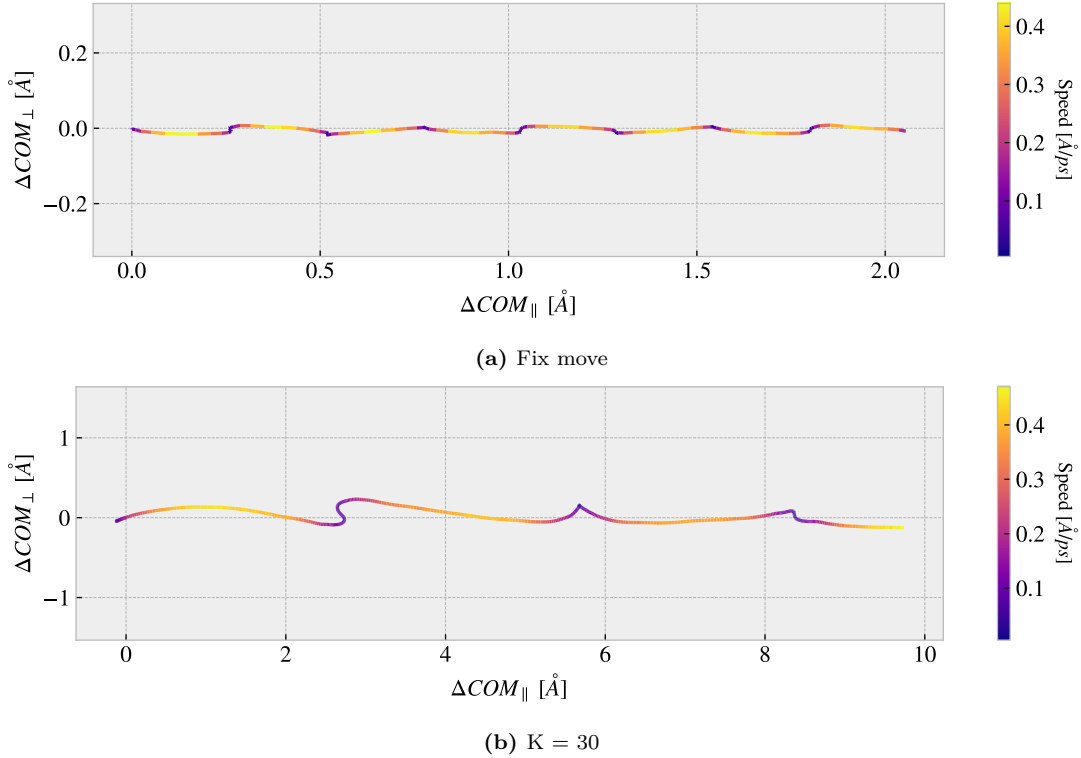


Figure 4: Center of mass relative position from start of drag phase in terms of axis parallel to drag direction ΔCOM_{\parallel} and axis perpendicular to drag direction ΔCOM_{\perp} . The colorbar denotes the absolute speed of the COM.

0.5.1.2 Defining metrics for dynamic and static friction

We are interested taking the comprehensive friction force time series dataset and reducing it into single metrics describing the dynamic and static friction respectively. The natural choice is to use the mean and max values.

Dynamic friction For the dynamic friction measurement we take the mean of the latter half of the data to ensure that the system has stabilised itself before taking the mean. For a full drag simulation of 400 Å we would thus base our mean value on the latter 200 Å drag. In figure 5a we have shown the friction force of the first 10 Å of drag together with a running mean with window length 50% of the corresponding data length. The final mean value estimate is indicated with red point at the end and we clearly observe that the length of sampling is insufficient since we get a negative friction force. Nonetheless, one approach to quantify the uncertainty of the final mean estimate is to consider the running mean. The more the running mean fluctuates the more uncertainty is associated with the final estimate.

We should not care for fluctuations in the initial part of the running mean curve as this is still including data from the beginning, where it might transition from static to dynamic friction. Only the running mean “close” to the ending should be considered for our uncertainty. From the Fourier analyse we concluded that longest period of any dominant oscillations is $\sim 71 \text{ Å}^{-1}$ corresponding to $\sim 35\%$ of the running mean window of 200 Å drag. Hence we use standard deviation of the final 35% of the running mean curve to approximate the uncertainty of the final mean value. By dividing with the final running mean we effectively calculate the relative error as shown in figure 5b. Naturally, we get a relative error of $\sim 257\%$ which corresponds with the mean value taking an unexpected negative value.

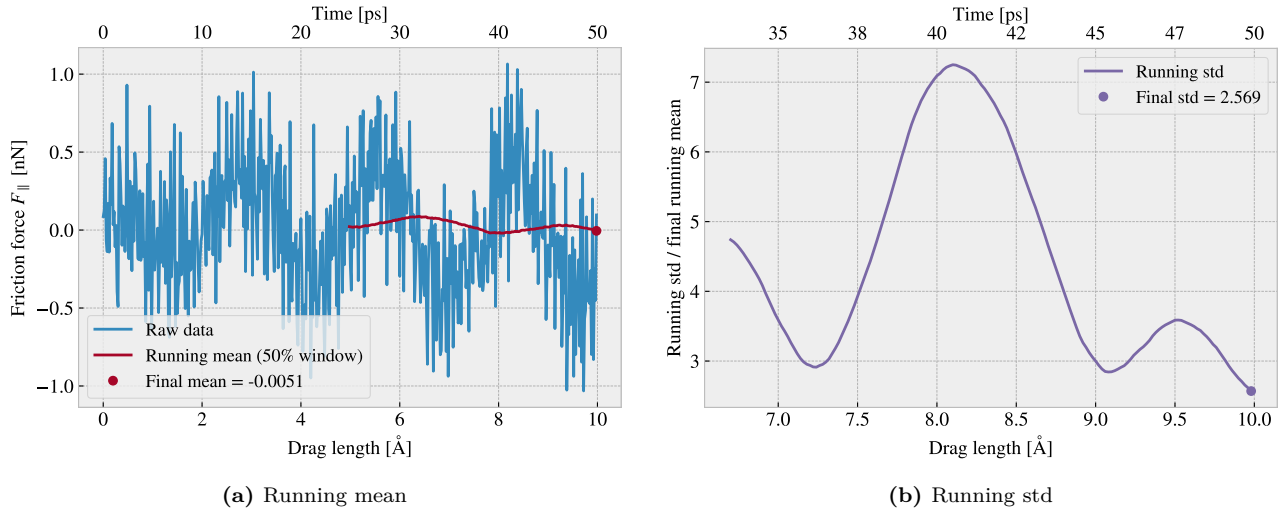


Figure 5: Running std

When we include the full 400 Å drag, such that std window actually matches with the longest period of oscillations expected from the data, we get a final relative error of $\sim 12\%$ as shown in fig 6. This is just at the limit for an acceptable error, but as we shall see later (refer to figure or something) this high error is mainly connected to the cases of low friction. When changing the simulation parameters, such that the mean friction evaluate to considerable higher values, the relative error drops to around (put in numbers). One explanation is that the oscillations in the running mean does not increase linearly with the magnitude of the friction, and hence the relative error might spike especially for the low friction cases.

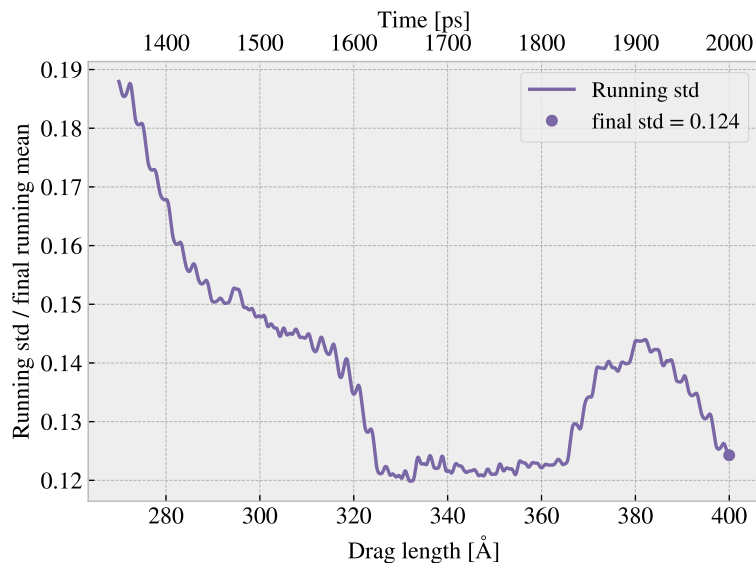


Figure 6: ...

Static friction The max value is the most obvious choice for addressing the static friction, even though that the definition of the static friction is a bit vague. At least when judging from the raw data in figure 1 we not see a textbook example of the static friction precursor (maybe include a classic static friction curve in the theory... I'm not completely sure what to expect here). Additionally the global max value does not always lie in the initial part of the simulation.

For a proper static friction evaluation we should increase force slowly and wait for the slip response. Here we drag quite fast making it difficult to assess the static response.

We investigate the placement of the max values, i.e. the drag length for which we measure the max friction force. We show the placement of the top three max values for different simulations with varying normal force in figure 7. We observe immediately that only a few top three max values is measured within a full slow period of ~ 71 Å. In fact many max values is measured just before the end of the simulation. This indicates that the naive approach of using the overall max value to describe the static friction coefficient might be a too naive approach. Another approach is to use the max value within a single period, but we do not really know if this period will be similar for all cut patterns and thus this might be limiting.

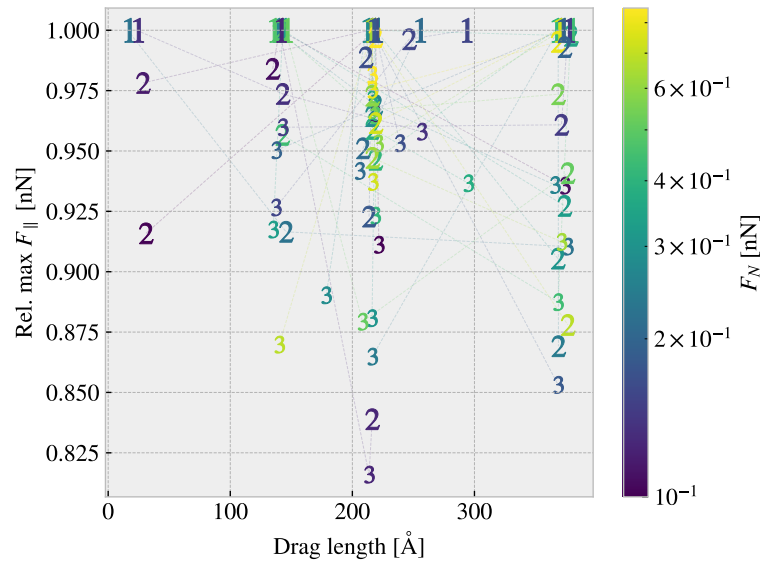
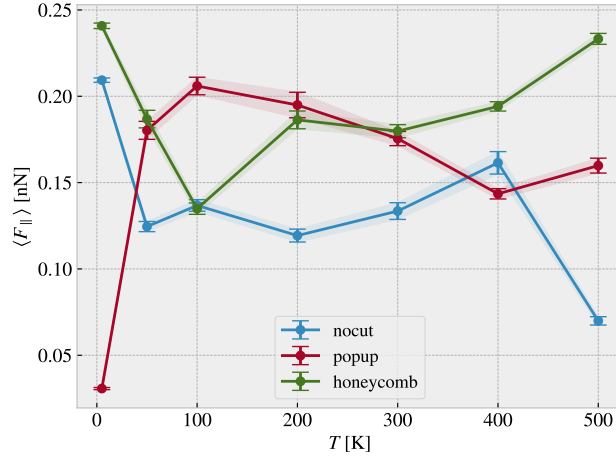
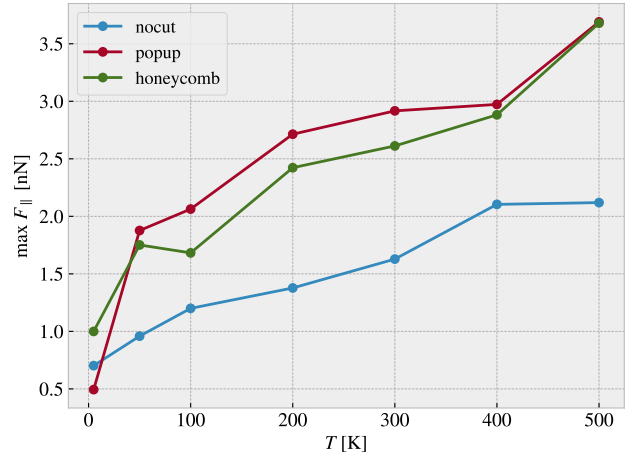


Figure 7: Distribution of top 3 max values for different normal force

0.5.1.3 Varying temperature, drag speed, spring constant and dt

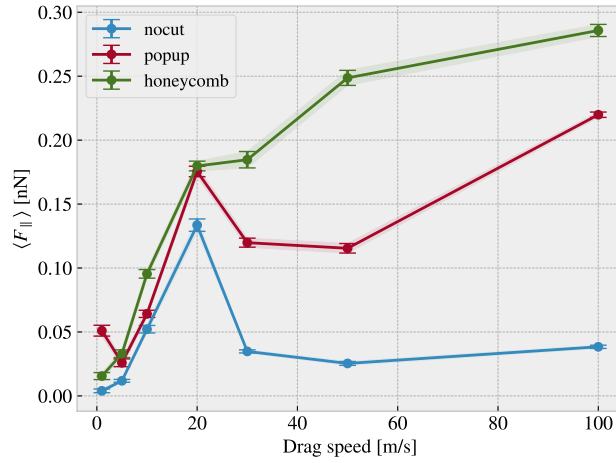


(a) mean friction

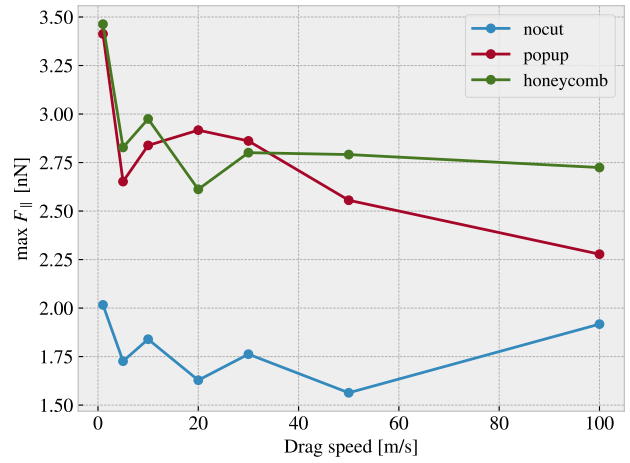


(b) max friction

Figure 8: Temperature

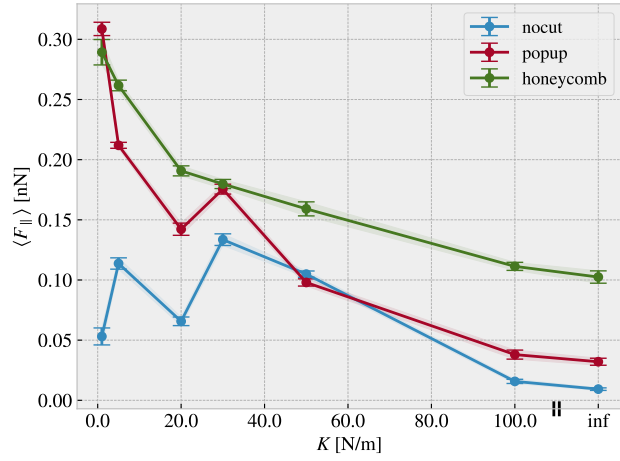


(a) mean friction

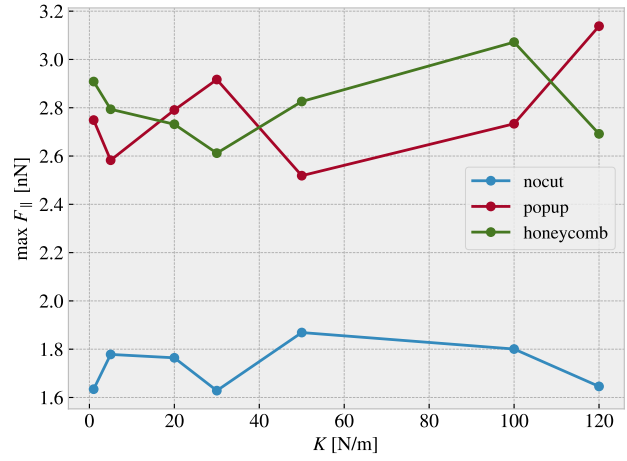


(b) max friction

Figure 9: Drag speed

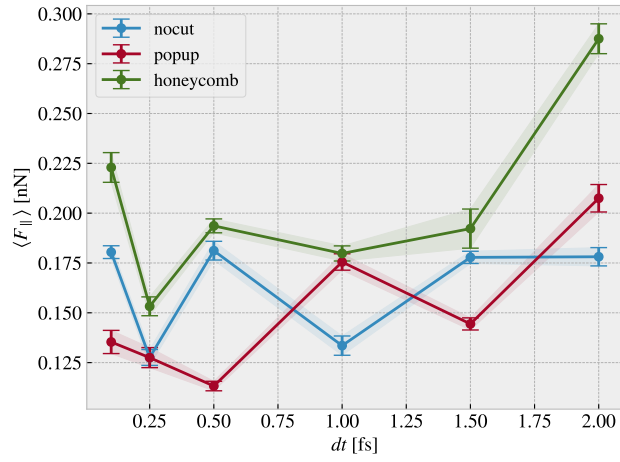


(a) mean friction

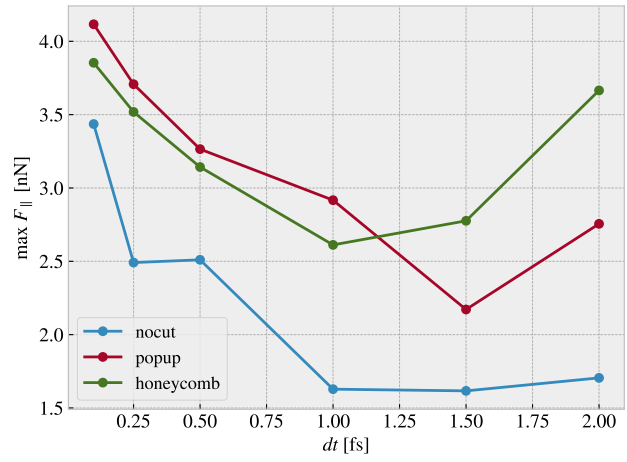


(b) max friction

Figure 10: Spring constant



(a) mean friction



(b) max friction

Figure 11: Timestep

0.5.1.4 Varying normal force and stretch

Multi stretch text

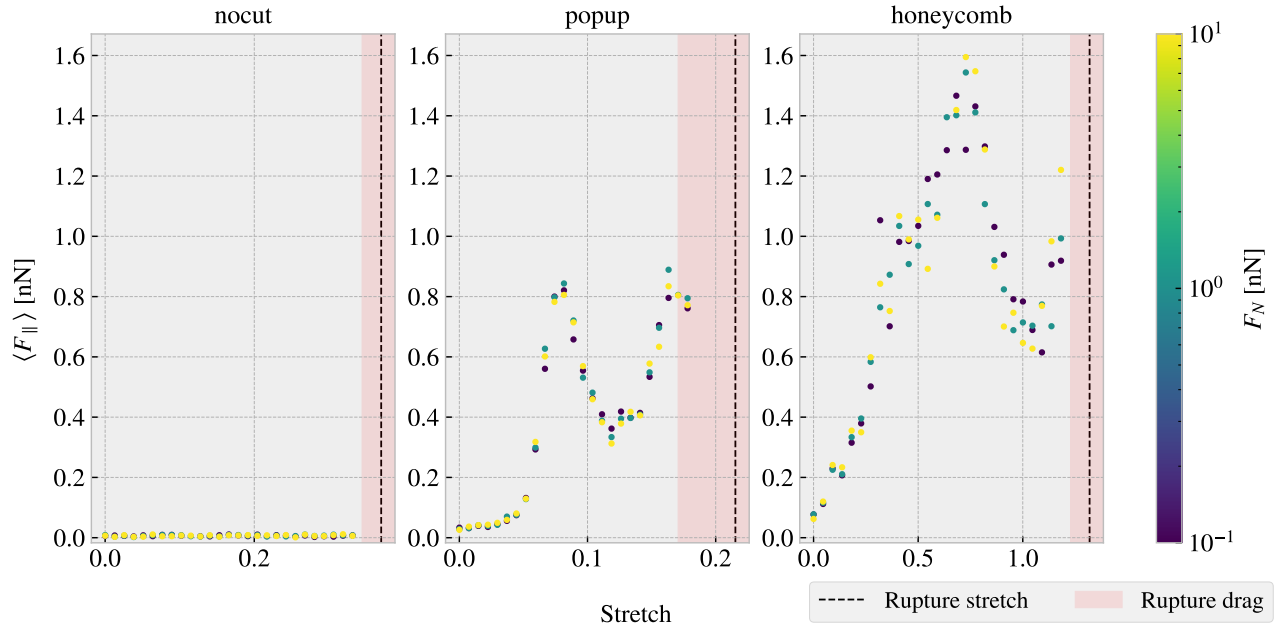


Figure 12: ...

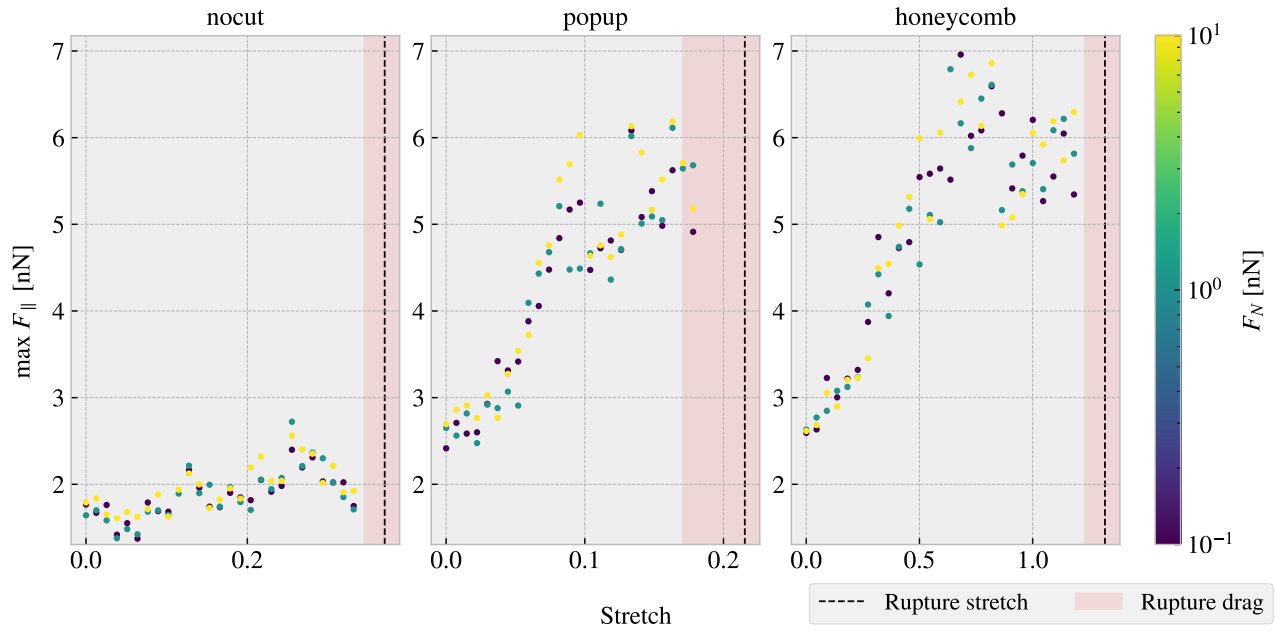


Figure 13: ...

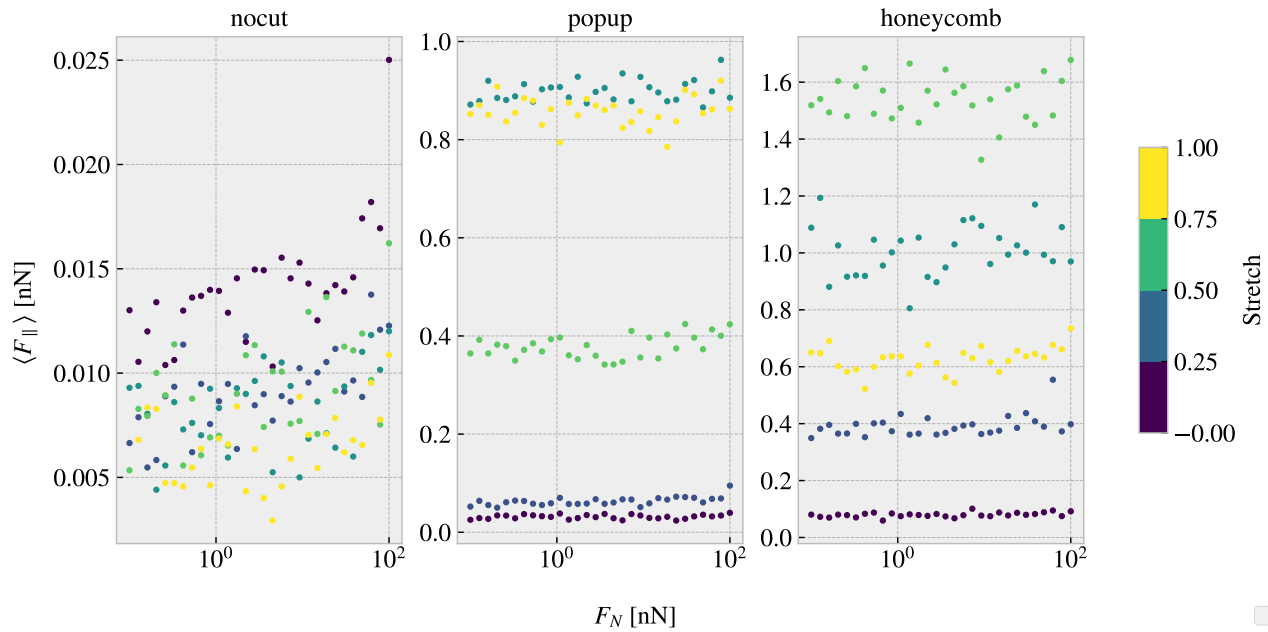


Figure 14: ...

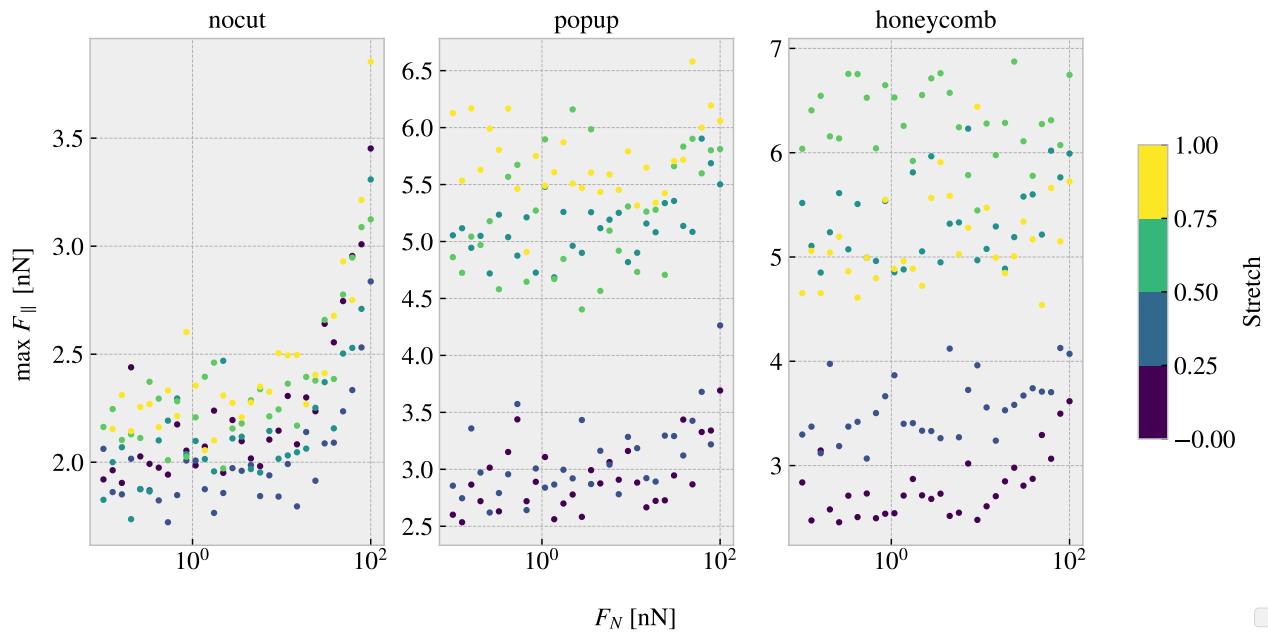


Figure 15: Colorbar is only fitted for the right plot (honeycomb)... this should be fixed. Should I have run a linear distribution of FN so I could plot it linear here also...?

Table 2: Mean friction coeff

nocut	$0.00009 \pm 1 \times 10^{-5}$	$0.00005 \pm 1 \times 10^{-5}$	$0.00004 \pm 1 \times 10^{-5}$	$0.00005 \pm 2 \times 10^{-5}$	
popup	$0.00005 \pm 3 \times 10^{-5}$	$0.00024 \pm 5 \times 10^{-5}$	$0.0002 \pm 2 \times 10^{-4}$	$0.0005 \pm 1 \times 10^{-4}$	$0.0003 \pm 2 \times 10^{-4}$
honeycomb	$0.00013 \pm 6 \times 10^{-5}$	$0.0006 \pm 3 \times 10^{-4}$	$0.0004 \pm 6 \times 10^{-4}$	$0.0007 \pm 6 \times 10^{-4}$	$0.0009 \pm 3 \times 10^{-4}$

Table 3: Max friciton coeff

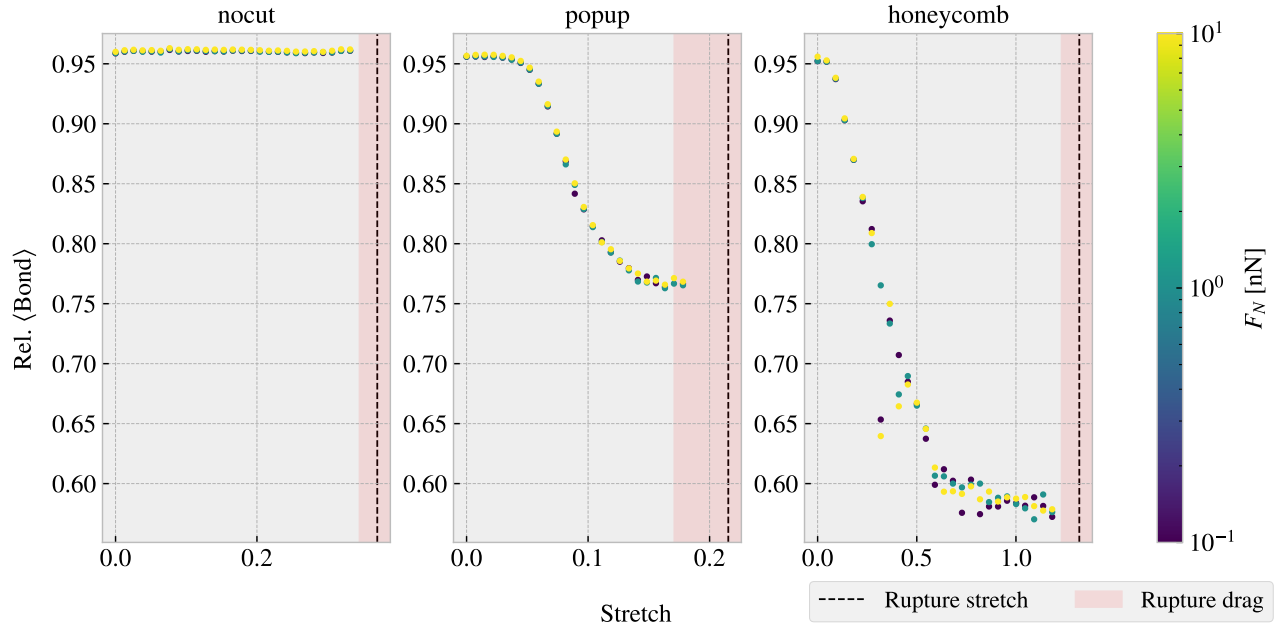
nocut	$0.0139 \pm 9 \times 10^{-4}$	$0.0083 \pm 7 \times 10^{-4}$	$0.010 \pm 1 \times 10^{-3}$	$0.0105 \pm 9 \times 10^{-4}$	
popup	$0.007 \pm 2 \times 10^{-3}$	$0.010 \pm 2 \times 10^{-3}$	$0.007 \pm 2 \times 10^{-3}$	$0.009 \pm 3 \times 10^{-3}$	$0.006 \pm 2 \times 10^{-3}$
honeycomb	$0.010 \pm 1 \times 10^{-3}$	$0.007 \pm 2 \times 10^{-3}$	$0.007 \pm 3 \times 10^{-3}$	$0.000 \pm 3 \times 10^{-3}$	$0.004 \pm 3 \times 10^{-3}$

Multi normal force The friction probably does not increase with normal force at an expected rate due to the fact the normal force is only applied on the pull blocks. Especially with the cutted sheet the tension drops such that the effective normal force on the inner sheet is not changing so much. By this theory the friction force vs. normal force on the pull graph look a bit more like expected.

When looking at the graphs for the PB the max friction is visually textbook linear, while the mean friction is a bit more linear but also with negativ coefficients.

0.5.1.5 Contact area

Show plots of contact area vs stretch and discuss the fact that friction actually increases while contact area drops. Is the conclusion that there might be another more dominant cause of the increasing friction.

**Figure 16**

Bibliography

- [1] E. Gnecco and E. Meyer, *Elements of Friction Theory and Nanotribology*. Cambridge University Press, 2015, [10.1017/CBO9780511795039](https://doi.org/10.1017/CBO9780511795039).
- [2] Bhusnan, *Introduction*, ch. 1, pp. 1–8. John Wiley & Sons, Ltd, 2013.
<https://onlinelibrary.wiley.com/doi/pdf/10.1002/9781118403259.ch1>.
<https://doi.org/10.1002/9781118403259.ch1>.
- [3] H.-J. Kim and D.-E. Kim, *Nano-scale friction: A review*, .
- [4] K. Holmberg and A. Erdemir, *Influence of tribology on global energy consumption, costs and emissions*, .
- [5] P. Z. Hanakata, E. D. Cubuk, D. K. Campbell and H. S. Park, *Forward and inverse design of kirigami via supervised autoencoder*, *Phys. Rev. Res.* **2** (Oct, 2020) 042006.